Photochemistry of a Trisilane Substituted by a Pendant *p*-Cyanostilbene Electron Acceptor Chromophore

Mark G. Steinmetz,* Chang Luo, and Gui Liu

Department of Chemistry, Marquette University, P.O. Box 1881, Milwaukee, Wisconsin 53201-1881

Received December 3, 1998

Photolysis of (*E*)-4-cyano-4′-(2-heptamethyltrisilanyl)stilbene (*E*)-**3** in a medium polarity solvent (CH_2Cl_2) results in efficient intramolecular electron transfer, which converts the initial π,π^* excited state (^{1}LE state) to the charge transfer (CT) excited state. The CT excited state fluorescesces, undergoes *E*,*Z* photoisomerization, and reacts with MeOH to produce hydrosilane **4** via Si−Si bond cleavage and protonation of the central silicon, as shown by deuterium labeling. The CT excited state assignments are consistent with the observed quadratic plots of $1/\Phi_f$ versus [MeOH] and $1/\Phi_{EZ}$ versus [MeOH], which indicate that both the initial ^{1}LE state and the CT excited state are quenched by MeOH, with the CT excited state serving as the emissive state and the state primarily responsible for the *E*,*Z* photoisomerization. Although biacetyl triplet sensitized photolysis results in efficient *E*,*Z* isomerization, quenching of direct photolyses by azulene shows (*Z*)-**3** is not a product of the lowest energy triplet excited state, populated from the CT state by back electron transfer. The azulene quenching also shows that hydrosilane **4** is formed from the same excited state that gives (*Z*)-**3**. The intermediacy of a complex of the CT excited state with MeOH accounts for the observed upward curvature in the plot of $1/\Phi_{SiH}$ vs 1/[MeOH]. The linear behavior of $\Phi_{EZ}/\Phi_{SiH} \times$ [MeOH] versus 1/[MeOH] further suggests that this complex reacts with uncomplexed MeOH to give hydrosilane **4**.

Introduction

Intramolecular charge transfer (CT) excited states figure prominently in the photochemistry of aryldisilanes[1,2] and related compounds having a disilanyl group directly linked to an electron deficient, π-conjugated chromophore.[2−4] The fluorescence of these electron donor−acceptor systems is often a composite of emissions of both the CT excited state and the π,π^* excited state (^{1}LE state) of the chromophore. The CT excited state can also undergo addition of an alcohol across the Si−Si bond to produce a hydrosilane photoproduct, in which case the orientation of the addition favors bond cleavage and proton transfer from alcohol to the internal silicon attached to the chromophore.[1a,3,4] The reaction is thought to involve initial nucleophilic interaction of the alcohol with the disilanyl group, which presumably becomes electron deficient in the CT excited state upon transfer of a σ electron to the π,π^* photoexcited electron acceptor chromophore.

In this paper we report on the photochemistry of a trisilane bearing a *p*-cyanostilbene chromophore attached as a pendant substituent. The same types of photoproducts are observed as reported previously for direct photolysis of disilanyl *p*-cyanostilbene (*E*)-**1**,[4] which gives (*Z*)-**1** and hydrosilane **2** upon reaction with alcohols.

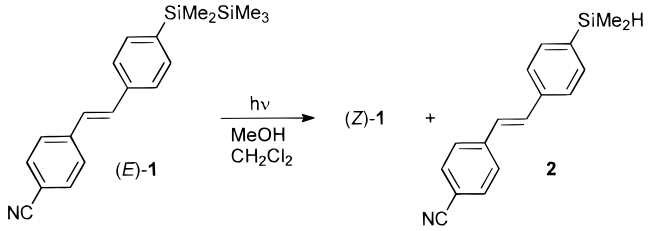

However, in the medium polarity solvent CH_2Cl_2, the *E*,*Z* photoisomerization of (*E*)-**3** originates from the CT excited state, whereas for (*E*)-**1** experiment supported a ^{1}LE state assignment. Our study of (*E*)-**3** has also provided some additional information on the mechanism of formation of hydrosilanes in alcohols. The evidence suggests that the CT excited state reacts with alcohols to form an intermediate complex. This complex can dissociate to regenerate ground state reactants, or it can undergo protonation and Si−Si bond cleavage to furnish hydrosilane.

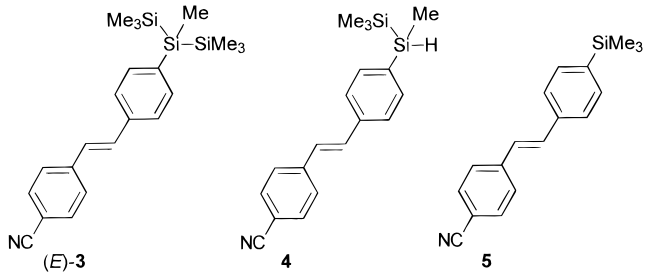

Results

Synthesis of (*E*)-4-Cyano-4′-(2-heptamethyltrisilanyl)stilbene (*E*)-3, Preparative Photolysis, Pho-

(1) (a) Kira, M.; Miyazawa, T.; Sugiyama, H.; Yamaguchi, M.; Sakurai, H. *J. Am. Chem. Soc.* **1993**, *115*, 3116. (b) Tajima, Y.; Ishikawa, H.; Miyazawa, T.; Kira, M.; Mikami, N. *J. Am. Chem. Soc.* **1997**, *119*, 7400.

(2) Steinmetz, M. G. *Chem. Rev.* **1995**, *95*, 1527.

(3) Steinmetz, M. G.; Yu, C.; Li, L. *J. Am. Chem. Soc.* **1994**, *116*, 932.

(4) Liu, G.; Heisler, L.; Li, L.; Steinmetz, M. G. *J. Am. Chem. Soc.* **1996**, *118*, 11412.

10.1021/jo982378+ CCC: $18.00
Published on Web 02/25/1999

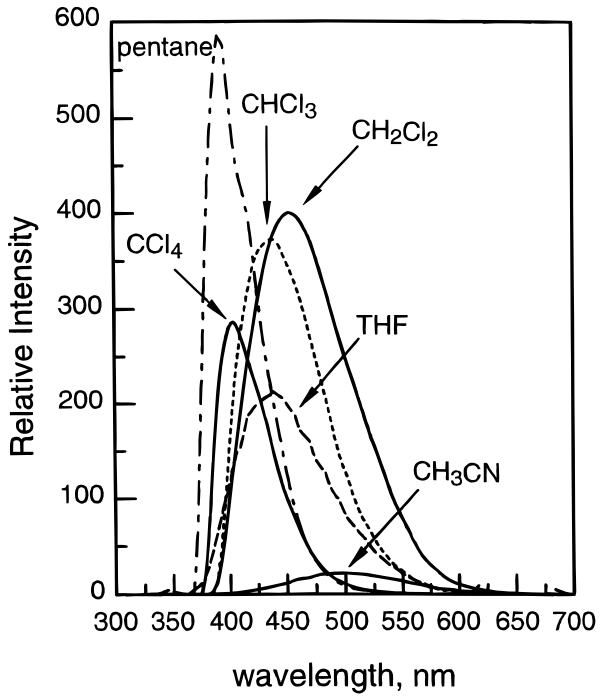

Figure 1. Fluorescence of 10^{-5} to 10^{-6} M (*E*)-**3** in various solvents.

toproducts, and Deuterium Labeling. Trisilanyl *p*-cyanostilbene (*E*)-**3** was synthesized by olefination of 4-(2-heptamethyltrisilanyl)benzaldehyde by *p*-tolunitrile phosphonate carbanion (Experimental Section). Pure (*E*)-**3** was obtained by column chromatography followed by recrystallization. (*E*)-**3** had to be protected from ambient light during all operations.

Preparative direct photolysis of 0.006 M (*E*)-**3** in MeOH utilizing Pyrex-filtered light of a 450-W medium-pressure mercury lamp gave, after column chromatographic separation, a 31% isolated yield of the pure trans isomer of hydrosilane **4** and a 20% isolated yield of the pure cis isomer of **4**. A fraction containing a 10.8:1 mixture of trans:cis isomers of **4** and a small amount of unreacted starting material was also obtained. The total yield of hydrosilane **4**, as a 2.9:1 trans:cis mixture, was 90%, and the yield of starting material (*E*)-**3** was 5%. The cis isomer of hydrosilane **4** was a secondary photoproduct, formed in negligible yield in all subsequent photolyses taken to low conversions.

Direct photolyses of (*E*)-**3** in CH_2Cl_2 containing MeOH gave both hydrosilane **4** and (*Z*)-**3**. The yields of these products varied with the concentration of MeOH (vide infra). In CH_2Cl_2 containing no MeOH, preparative photolysis of 0.005 M (*E*)-**3** gave (*Z*)-**3** as the sole product. Pure (*Z*)-**3** was isolated in 67% yield along with 29% yield of recovered reactant after column chromatography of the photolysate.

Direct photolysis of 0.01 M (*E*)-**3** in MeOD as the solvent gave Si-D labeled hydrosilane **4** according to ^{2}H NMR spectroscopy, and no deuterium was detected in (*E*)-**3**. GC-MS data showed that the extent of the monodeuteration of **4** was 98%, based on the M − 15 fragment ion. With 3 M MeOD in CH_2Cl_2 as the solvent, **4** was found to be 97% monodeuterated.

Fluorescence Studies. Fluorescence spectra of 10^{-5} to 10^{-6} M solutions of (*E*)-**3** in solvents of varying polarity are shown in Figure 1, and absorption and fluorescence data for the complete set of solvents examined are collected in Table 1. These data were used to construct solvatochromic plots from which the dipole moments of the ^{1}LE and CT states could be estimated. A Lippert−Mataga[5] plot (not shown) of the Stokes shift $\nu_a - \nu_f$ versus the solvent polarity parameter $\Delta f = (\epsilon - 1)/(2\epsilon + 1) - (n^2 - 1)/(2n^2 + 1)$, where ϵ and n are solvent dielectric constant and refractive index, shows two slopes with a common intercept. For pentane, Bu_2O, and Et_2O the slope is 4849 ± 728 $cm^{-1}/\Delta f$ ($R^2 = 0.9889$), whereas for the halogenated solvents and CH_3CN the slope is 16140 ± 1726 $cm^{-1}/\Delta f$ ($R^2 = 0.9888$). The solvent THF deviated and was not included in either correlation. The slopes of the correlations are proportional to $\Delta\mu^2$, where $\Delta\mu$ is the difference in ground and excited state dipole moments. Since the steeper slope likely corresponds to the solvent polarity induced shift of the CT emission, the calculated dipole moments are assigned $\Delta\mu_{CT} = 16$ D and $\Delta\mu_{LE} = 9$ D, where it is assumed the same molecular dimensions ($\rho = 5.43$ Å[6]) apply to (*E*)-**3** as found for 4′-cyano-4-dimethylaminostilbene (DCS).

Table 1. Absorption and Emission Maxima of (*E*)-3

solvent	$\Delta f(\epsilon,n)$	$(\epsilon - 1)/(\epsilon + 2)$	λ_a/nm	ϵ/$M^{-1}cm^{-1}$	λ_f/nm
pentane	0.001	0.219	335	45 400	393
Bu_2O	0.096	0.409	337	42 800	402
Et_2O	0.167	0.516	335	57 500	407
THF	0.210	0.687	336	37 100	437
CCl_4	0.010	0.291	341	55 700	404
$CHCl_3$	0.148	0.559	340	37 900	438
CH_2Cl_2	0.217	0.726	340	39 700	453
CH_3CN	0.305	0.921	335	50 000	491

Estimates of dipole moments which take into account polarization effects can be made by plotting fluorescence maxima ν_f against $(\epsilon - 1)/(\epsilon + 2)$, according to eq 1[7,8]

$$\nu_f = -\frac{2}{hc\rho^3}\left[(\mu_e^\circ - \mu_g)\mu_e^\circ\left(\frac{\epsilon - 1}{\epsilon + 2}\right) - \frac{1}{2}(\mu_e^\circ - \mu_g)^2\left(\frac{n^2 - 1}{n^2 + 2}\right)\right] + \text{constant}' \quad (1)$$

(Figure 2). As noted previously,[4] the term $0.5(n^2 - 1)/(n^2 + 2)$ is approximately constant. Two correlations are observed with slopes of −2787 ± 79 ($R^2 = 0.9996$) and −6799 ± 462 ($R^2 = 0.9954$), from which the term $\mu_e^\circ(\mu_e^\circ - \mu_g)$ is calculated to be 45 and 109 D[2]. The lower limit estimates of the dipole moments of the solvent-free molecule in the CT and ^{1}LE states are 10 and 7 D, respectively, taking $\mu_g = 0$. The ^{1}LE estimate is comparable to $\mu_e^\circ = 6$ D previously found[4] for monotrimethylsilyl *p*-cyanostilbene **5** (see Figure 2), which shows only a single correlation for the series of solvents.

Quantum yields of fluorescence and singlet excited state lifetimes of (*E*)-**3** are summarized in Table 2 along with data previously obtained[4] for disilane (*E*)-**1** and monosilane **5**. Comparison of the measured quantum yields of fluorescence (Φ_f) to quantum yields for formation of (*Z*)-**3** (Φ_{EZ}, vide infra) in CH_2Cl_2 suggest that the former are systematically too high by ca. 7−20%. Excited state lifetimes of (*E*)-**3**, determined by single photon

(5) (a) Lippert, V. E. Z. *Naturforsch.* **1955**, *10a*, 541. (b) Mataga, N.; Kaifu, Y.; Koizumi, M. *Bull. Chem. Soc. Jpn*, **1955**, *28*, 690.
(6) Lapouyade, R.; Czeschka, K.; Majenz, W.; Rettig, W.; Gilabert, E.; Rulliere, C. *J. Phys. Chem.* **1992**, *96*, 9643.
(7) Liptay, W. *Z. Naturforsch.* **1965**, *20a*, 1441.
(8) Létard, J.-F.; Lapouyade, R.; Rettig, W. *J. Am. Chem. Soc.* **1993**, *115*, 2441.

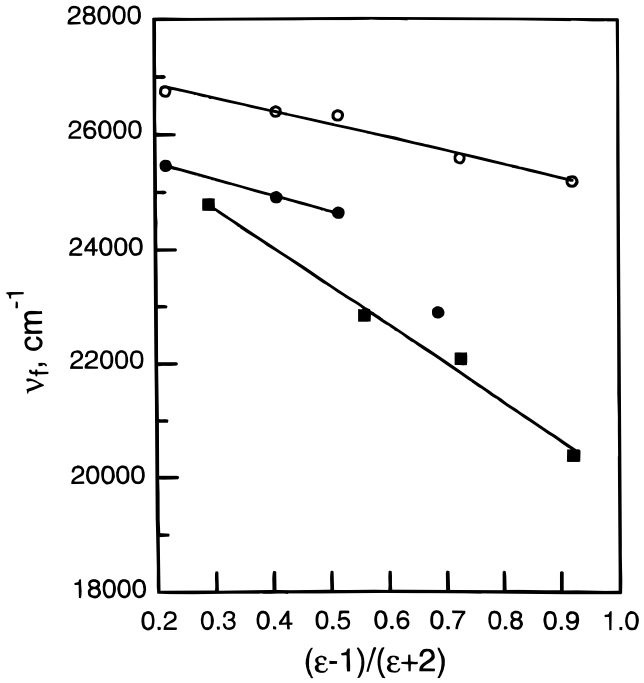

Figure 2. Solvatochromic plot of ν_f vs $(\epsilon - 1)/(\epsilon + 2)$ for trisilane (*E*)-**3** (■, halocarbons and CH_3CN; ●, ethers and pentane) and for monosilane (*E*)-**5** (○).

Table 2. Quantum Yields of Fluorescence and *E,Z* Isomerization and Excited State Lifetimes

	trisilane (*E*)-**3**		disilane (*E*)-**1**		monosilane **5**[a]	
solvent	Φ_f (τ, ns)	$\Phi(E,Z)$	Φ_f (τ, ns)	$\Phi(E,Z)$	Φ_f	$\Phi(E,Z)$
pentane	0.21 (0.4)	0.248	0.10[a] (0.3)	0.41[a]	0.031	0.38
THF	0.087 (nd[b])	0.0551	nd[b]	nd	nd	nd
CH_2Cl_2	0.79 (1.6)	0.167	0.20[a] (0.5[a])	0.55[a]	0.023	0.40
CH_3CN	0.039 (0.4)	0.0054	0.003[a] (<0.1)	0.012[a]	0.016	0.39

[a] From ref 4. [b] Not determined.

counting, are considerably longer in deoxygenated CH_2Cl_2 than in other solvents such as pentane or CH_3CN. In all cases the fluorescence decays appeared to be monoexponential and did not vary significantly with change in excitation or emission wavelengths.

The steady state fluorescence of 10^{-4} M (*E*)-**3** was found to be quenched by MeOH in CH_2Cl_2. The standard Stern−Volmer plot of Figure 3 shows upward quadratic curvature, obeying the equation $\Phi_f^\circ/\Phi_f = 1 + (a + b)$[MeOH] + (*ab*)[MeOH]^2 with $a = 0.14 \pm 0.08$ and $b = 0.49 \pm 0.19$ ($R^2 = 0.9975$) where a and b are $k_q\tau$ values (M^{-1}) for quenching of two different excited states (^{1}LE and CT) with the higher energy excited state initially populated and the lower energy excited state (CT) the emitter. Fluorescence quenching by MeOH in pentane (not shown) gives a linear Stern−Volmer plot with $k_q\tau = 0.50 \pm 0.01$ ($R^2 = 0.9988$). In these experiments the solvent was not deaerated. The error limits correspond to one standard deviation.

The excited state lifetimes τ in deaerated CH_2Cl_2 were found to decrease with increasing MeOH concentration. The experimental functional dependence was observed to be linear (Figure 4, $R^2 = 0.9947$), obeying $1/\tau = 1/\tau^\circ + k_q$[MeOH] with $k_q = 0.50 \pm 0.03 \times 10^9$ s^{-1} and $1/\tau^\circ = 0.59 \pm 0.08 \times 10^9$ s^{-1}. From the slope/intercept $k_q\tau = 0.85 \pm 0.09$. Errors are one standard deviation.

Quantum Yields of Photoproducts. Quantum yields of (*Z*)-**3** (Φ_{EZ}) and hydrosilane **4** (Φ_{SiH}) were determined

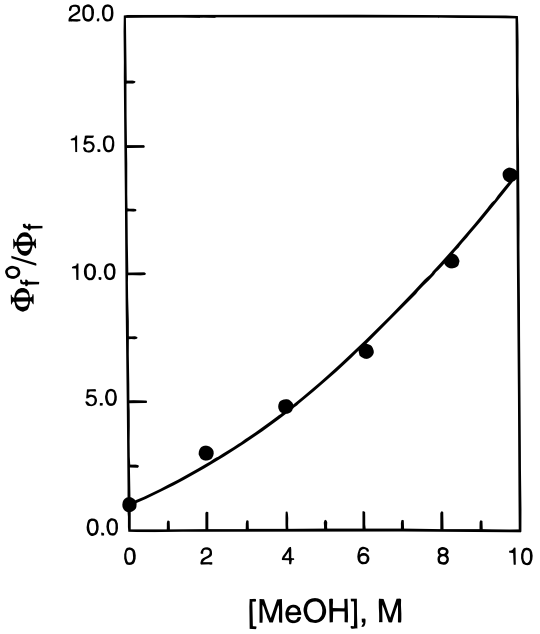

Figure 3. Relative quantum yields of fluorescence of (*E*)-**3** for a series of MeOH concentrations in CH_2Cl_2 as the solvent.

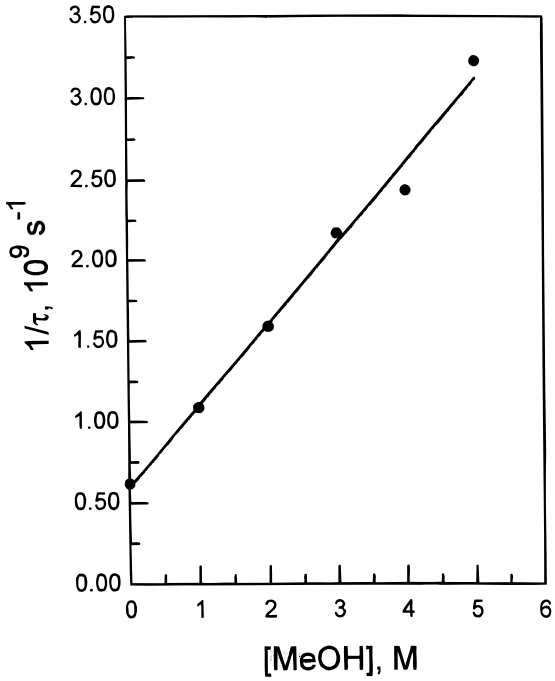

Figure 4. Fluorescence decay rates for a series of MeOH concentrations in CH_2Cl_2 as solvent.

at low conversions for 340 nm direct photolyses of 0.01 M (*E*)-**3** in deoxygenated solvents utilizing ferrioxalate actinometry. In the absence of MeOH, hydrosilane **4** was not observed. The values for Φ_{EZ} in various solvents are summarized in Table 2.

The *E,Z* photoisomerization of (*E*)-**3** was found to be quenched by MeOH in CH_2Cl_2. The Stern−Volmer plot of $1/\Phi_{EZ}$ versus [MeOH] for (*E*)-**3** is not linear, but displays upward quadratic curvature (Figure 5). An excellent nonlinear least-squares fit ($R^2 = 0.9986$) was obtained for the equation $1/\Phi_{EZ} = (4.88 \pm 0.63) + (5.32 \pm 0.87)$[MeOH] + (1.12 ± 0.20)[MeOH]^2. The quadratic behavior implies that two excited states are quenched

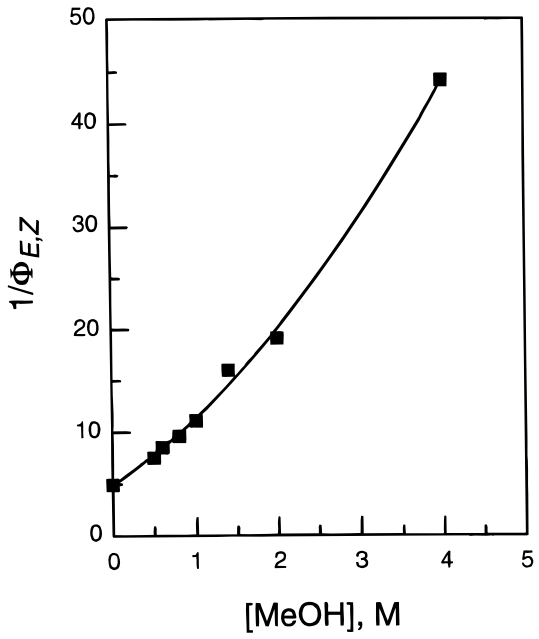

Figure 5. Quenching of the *E*,*Z* photoisomerization of (*E*)-**3** by MeOH in CH_2Cl_2.

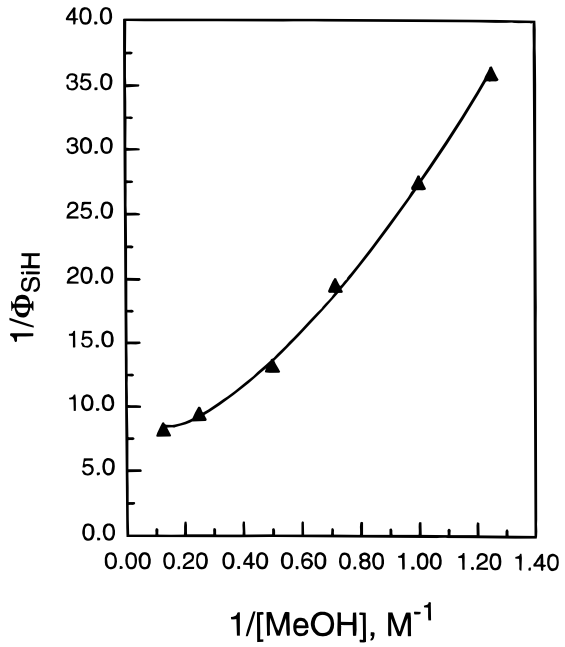

Figure 6. Double reciprocal plot of quantum yields of hydrosilane **4** and the concentration of MeOH in CH_2Cl_2.

by the MeOH. The higher energy state (^{1}LE) would be initially populated, and the lower energy state (CT) would be the one which isomerizes to (*Z*)-**3**, as shown in Scheme 1. According to Scheme 1, eq 2 should hold,[9] where parameters *a* and *b* are Stern−Volmer constants $k_q\tau$ (M^{-1}) for the two states that are quenched and $d = \Phi^\circ_{EZ}$ at zero [MeOH]. The following parameters are calculated from the quadratic fit: $d = 0.20 \pm 0.03$, $a = 0.29 \pm 0.01$, and $b = 0.80 \pm 0.04$.

$$\frac{1}{\Phi_{EZ}} = \frac{1}{d} + \frac{(a+b)}{d}[\mathrm{MeOH}] + \frac{ab}{d}[\mathrm{MeOH}]^2 \qquad (2)$$

$$d = \Phi^\circ_{E,Z} = \phi_{12}\phi_{r2} \qquad a \text{ or } b = k_{q1}\tau_1 \text{ or } k_{q2}\tau_2$$

$$\frac{1}{\Phi_{SiH}} = \left[\left(ab + (a+b)\frac{1}{[\mathrm{MeOH}]} + \frac{1}{[\mathrm{MeOH}]^2}\right)\left(c + \frac{1}{[\mathrm{MeOH}]}\right)\right] \Big/ \left(m\frac{1}{[\mathrm{MeOH}]}\right) \qquad (3)$$

$$c = k_{qc}\tau_c \qquad m = \phi_{12}bc$$

$$\frac{\Phi_{EZ}}{\Phi_{SiH}}[\mathrm{MeOH}] = \frac{d}{m}\left(c + \frac{1}{[\mathrm{MeOH}]}\right) \qquad (4)$$

Quantum yields Φ_{SiH} for hydrosilane **4** were found to increase with increasing concentration of MeOH in CH_2Cl_2. The upward curvature of the double reciprocal plot of $1/\Phi_{SiH}$ versus 1/[MeOH] (Figure 6) was interpreted in terms of a mechanism involving complexation of the CT state by MeOH to produce an intermediate (Scheme 1). Reaction of the intermediate complex with MeOH in a second bimolecular step would then furnish hydrosilane **4**. According to this assumed mechanism, the functional dependence of the plot should obey eq 3. Furthermore, a plot of $[\Phi_{EZ}/\Phi_{SiH}][\mathrm{MeOH}]$ versus 1/[MeOH] should be linear (eq 4). Such a linear dependence was found (Figure 7) with an intercept of 0.282 ± 0.073 M and slope of 2.15 ± 0.09 M^2 ($R^2 = 0.9974$). From the ratio of intercept/slope parameter, $c = 0.13 \pm 0.04$ M^{-1}, which is the $k_q\tau$ value for bimolecular reaction of the complex with MeOH to form hydrosilane **4**. With parameters *a*, *b*, and *c* determined above, the nonlinear least-squares fit of the data in Figure 6 using eq 3 gives parameter $m = 0.097 \pm 0.001$ M^{-2} ($R^2 = 0.9992$). A similar value for parameter *m* is alternatively obtained from the intercept or slope of eq 4. Since parameter $m = \phi_{12}bc$, the efficiency for the electron transfer converting the ^{1}LE state to the CT excited state (ϕ_{12}) is calculated to be 0.93 ± 0.33.

Scheme 1

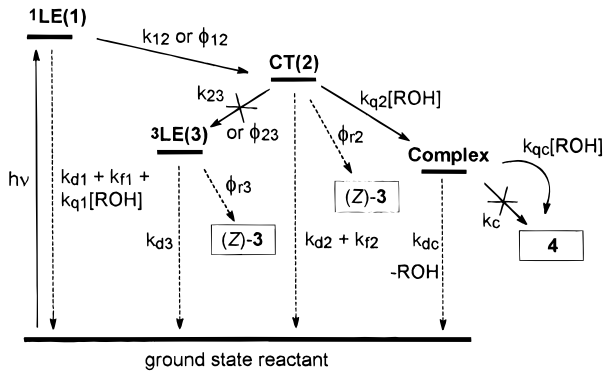

Equation 3 will have a shallow minimum at ca. 7 M MeOH where $\Phi_{max} = 0.12$. The measured quantum yields for hydrosilane **4** showed little variation when the concentration of MeOH is doubled from 4 to 8 M MeOH in CH_2Cl_2, i.e., $\Phi_{SiH} = 0.11$ and 0.12.

Biacetyl Sensitization and Azulene Quenching. An azulene quenching study was performed to determine whether (*Z*)-**3** is produced in the ^{3}LE state populated by back electron transfer from the higher energy CT state (Scheme 1). This alternative would be accommodated by eq 2 by redefining parameter *d* as $\Phi^\circ_{EZ} = \phi_{12}\phi_{23}\phi_{r3}$ and

(9) (a) Shetlar, M. D. *Mol. Photochem.* **1973**, *5*, 311. (b) Wagner, P. J. Chapter 4. In *Creation and Detection of the Excited State*; Lamola, A. A., Ed.; Marcel Dekker: New York, 1971.

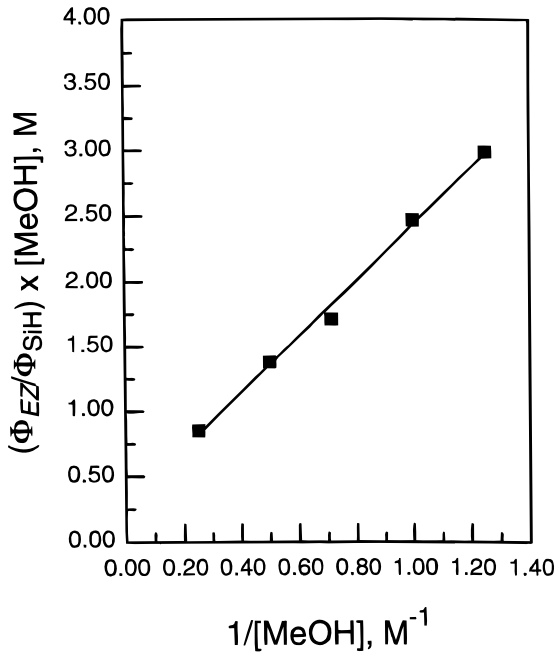

Figure 7. Dependence of the (*Z*)-**3**/**4** product ratio × [MeOH] on 1/[MeOH] in CH_2Cl_2 as the solvent.

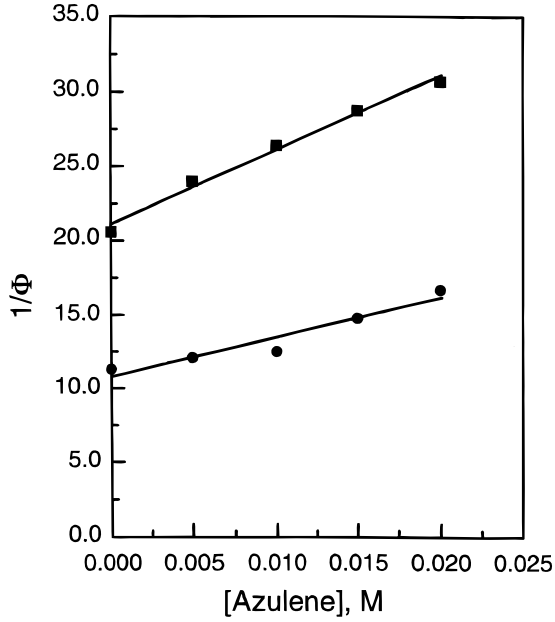

Figure 8. Quenching of the *E,Z* photoisomerization and the formation of hydrosilane **4** by azulene in 2 M MeOH in CH_2Cl_2.

thus would be indistinguishable from *E,Z* photoisomerization in the CT excited state on the basis of the data in Figure 5. The triplet excited state of (*E*)-**3** undergoes *E,Z* photoisomerization efficiently upon biacetyl ($E_T = 56$ kcal mol^{-1}) sensitized photolysis in CH_2Cl_2, and $\Phi_{EZ} = 0.42$. With 5 M MeOH present, sensitized photolysis gives no detectable hydrosilane **4** at 20% conversion. Since the quantum yield of (*Z*)-**3** remains unchanged ($\Phi_{EZ} = 0.41$), the triplet-sensitized *E,Z* photoisomerization is not quenched by the MeOH.

Quantum yields of (*Z*)-**3** and hydrosilane **4** were determined for various concentrations of azulene quencher at a constant 2 M MeOH in CH_2Cl_2. To ensure that 0.01 M (*E*)-**3** and not 0.005−0.02 M azulene absorbed the light, the excitation wavelength for the photolyses was shifted from 340 to 380 nm. Quantum yields without azulene measured at this longer wavelength were unchanged from those determined at 340 nm. At 380 nm, Φ_{EZ} and Φ_{SiH} are 0.048 and 0.088, respectively, compared to 0.052 and 0.076 at 340 nm. As shown by the Stern−Volmer plots in Figure 8, both (*Z*)-**3** and hydrosilane **4** are quenched by azulene. The plots for both products show good linearity, and the quenching constants from the slope/intercept ratios were found to be identical within experimental error: $k_q\tau$ of 23.6 ± 1.8 M^{-1} for (*Z*)-**3** and 25.0 ± 5.4 for **4**. These results suggest that both the *E,Z* photoisomerization and formation of hydrosilane **4** originate from the same excited state, which we assign as the CT excited state. From the singlet excited state lifetime in 2 M MeOH in CH_2Cl_2 of 0.63 ns, the bimolecular rate constant for quenching by azulene is calculated to be $k_q = 4 \times 10^{10}$ M^{-1} s^{-1}.

Discussion

The fluorescence of (*E*)-**3** appears to be a combination of ^{1}LE and CT excited state emissions with the latter dominating in solvents of intermediate or higher polarity. The fluorescence appearing at relatively short wavelength in pentane undergoes pronounced red shifts in $CHCl_3$, CH_2Cl_2, and CH_3CN as the solvents, whereas considerably smaller solvent polarity induced shifts are observed for Bu_2O and Et_2O. When the fluorescence maxima are plotted against the solvent polarity index $(\epsilon - 1)/(\epsilon + 1)$ (eq 1 and Figure 2), two correlations are observed, consistent with contributions by two emissive excited states. The correlation with the steeper slope and, hence, larger dipole moment, we assign to CT excited state, whereas the less polar excited state, assigned to the ^{1}LE state, has a similar slope and dipole moment as the previously investigated monotrimethylsilyl-substituted *p*-cyanostilbene **5**,[4] which exibits only a single correlation for pentane, Bu_2O, Et_2O, CH_2Cl_2, and CH_3CN (Figure 2). Except for the deviation of THF from the ether correlation line and the observance of a more intense emission in CH_3CN, the results are similar to those for (*E*)-**1**, for which the ^{1}LE and CT dipole moments of the solvent free molecule ($\mu_e°$) are 6 and 8 D,[4] as compared to 7 and 10 D for (*E*)-**3**. Use of the Lippert−Mataga equation[5] gives a difference in ground and excited state dipole moments of 16 D, which is comparable to the value of 14.6 D found for 4-(dimethylamino)-4′-cyanostilbene (DCS).[6]

The fluorescence of (*E*)-**3** in CH_2Cl_2 is quenched by MeOH. The upward quadratic curvature in the corresponding Stern−Volmer plot (Figure 3) is consistent with the above assignment of the CT excited state as the primary emissive excited state in this medium-polarity solvent. The quadratic curvature can be ascribed to quenching of both the ^{1}LE and CT excited states with the lower energy CT excited state the emissive state. Figure 3 contrasts with the linear Stern−Volmer plot for (*E*)-**1**,[4] which reflected quenching of the residual ^{1}LE component of a dual emission. In that case the CT component of the fluorescence was almost completely quenched at low concentrations of MeOH.

Quantum yields of *E,Z* photoisomerization of (*E*)-**3** show a Stern−Volmer quadratic dependence on MeOH concentration (Figure 5) similar to that of the fluorescence quantum yields in CH_2Cl_2. Like the fluorescence,

the *E,Z* photoisomerization in CH_2Cl_2 is thus assigned to the CT excited state. Linear Stern−Volmer quenching by MeOH in CH_2Cl_2 would be expected for *E,Z* photoisomerization in the ^{1}LE state, as was observed for (*E*)-**1**.[4] The pair of Stern−Volmer quenching constants $k_{q1}\tau_1$ and $k_{q2}\tau_2$, obtained by fitting eq 2 to the data in Figure 5, have relative magnitudes similar to those obtained from the dependence of relative quantum yields of fluorescence on [MeOH] (Figure 3), but the agreement is not quantitative, possibly because the CH_2Cl_2 solvent was not deaerated prior to the fluorescence measurements. Quantitative agreement is found with the $k_{q2}\tau_2$ value of 0.85 M^{-1} that is obtained from Figure 4 using single photon counting techniques to study the quenching of the CT excited state fluorescence by MeOH in deaerated CH_2Cl_2.

No curvature was evident in Figure 4 over the 1−10 M range of concentrations of MeOH in CH_2Cl_2 used in our study. Pronounced curvature in such plots has been observed for trapping of carbenes by low concentrations of alcohols in isooctane and in acetonitrile.[10] Upward curvature was attributed to quenching by hydrogen-bonded oligomers, which increase in concentration with increasing concentration of alcohol, whereas downward curvature was ascribed to selective quenching by monomer. The pseudo-first-order behavior in Figure 4 indicates that bulk [MeOH] sufficiently accounts for the quenching of the CT excited state of (*E*)-**3**.

The quenching of the fluorescence and *E,Z* photoisomerization of (*E*)-**3** by MeOH is accompanied by the formation of hydrosilane **4**. In the absence of MeOH the hydrosilane is not observed for any of the solvents in Table 2, suggesting that significant amounts of **4** are not formed via disproportionation of silyl radicals produced upon Si−Si bond dissociation. The high incorporation of one deuterium from MeOD into hydrosilane **4** as Si-D instead implies a mechanism involving nucleophilic attack by MeOH at a terminal trimethylsilyl group and proton (deuteron) transfer to the central silicon upon cleavage of the Si−Si bond. 4-(Methoxydimethylsilyl)-4′-cyanostilbene was never detected in photomixtures. Thus, nucleophilic attack by MeOH at the central silicon was not considered to be a significant process. Nucleophilic interaction of the solvent may be important in the apparent quenching of both fluorescence and *E,Z* photoisomerization by THF and CH_3CN, as shown by comparison of quantum yields to those measured for CH_2Cl_2 in Table 2.

The experimental dependence of quantum yields of hydrosilane **4** on the concentration of MeOH can be interpreted in terms of the mechanism in Scheme 1, whereby alcohol nucleophilically interacts with the CT excited state to produce an intermediate complex. This complex could dissociate to regenerate reactants, or it could undergo subsequent proton transfer with cleavage of the Si−Si bond to furnish the hydrosilane product. In principle, the proton transfer converting the complex to hydrosilane could be intramolecular, if the geometry is favorable, although bimolecular proton transfer from uncomplexed alcohol would seem more likely, if the proposed complex adopts a geometry similar to that of **6**, with an incipient disilanyl leaving group anti to the

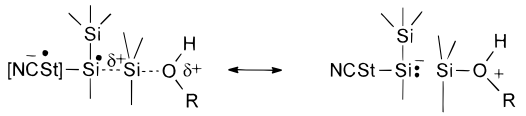

6

alcohol. Steady state kinetic treatment taking into account the additional intramolecular proton transfer pathway (k_c in Scheme 1) furnishes eq 5.[11] The product ratio (*Z*)-**3**/hydrosilane **4** multiplied by [MeOH] is expressed by eq 6. Experimentally, the linear plot of the data in Figure 7 suggests that intramolecular proton transfer in the complex is negligible (parameter $n = \phi_{12}bk_c\tau_c \approx 0$ in eq 5 or 6) such that hydrosilane **4** is formed primarily via bimolecular proton transfer from uncomplexed MeOH. Equations 5 and 6 then reduce to the simpler expressions, eqs 3 and 4 (Results Section).

$$\frac{1}{\Phi_{SiH}} = \frac{\left(ab + (a+b)\frac{1}{[\mathrm{MeOH}]} + \frac{1}{[\mathrm{MeOH}]^2}\right)\left(c + \frac{1}{[\mathrm{MeOH}]}\right)}{m\frac{1}{[\mathrm{MeOH}]} + n\frac{1}{[\mathrm{MeOH}]^2}} \qquad (5)$$

$$m = \phi_{12}bc \qquad n = \phi_{12}bk_c\tau_c$$

$$\frac{\Phi_{EZ}}{\Phi_{SiH}}[\mathrm{MeOH}] = \frac{d\left(c + \frac{1}{[\mathrm{MeOH}]}\right)}{m + n\frac{1}{[\mathrm{MeOH}]}} \qquad (6)$$

The efficiency for intramolecular electron transfer (ϕ_{12}) in CH_2Cl_2 as the solvent is found to be 0.93 from fitting of eqs 2−4 to the experimental data (Results Section). Equations 2−4 for trisilanyl derivative (*E*)-**3** assume ϕ_{12} and k_{12} do not vary significantly with solvent polarity, as would be expected for a highly efficient electron transfer step. In contrast, the electron transfer in disilane (*E*)-**1** was considered less efficient and subject to a solvent polarity effect, such that $k_{12} \propto$ [MeOH], consistent with a linear relationship found between $E_T(30)$ and ln[MeOH] above 0.3 M MeOH in CH_2Cl_2.[4]

Previous mechanisms propose that hydrosilanes are formed via a single act of quenching of the CT excited state of disilanylarenes[1a] and (*E*)-**1**[4] by alcohols. These mechanisms, which invoke the aforementioned solvent polarity dependent electron transfer rate constant k_{12} ($k_{12} \propto$ [ROH]^4 or variants[1a]), account for the observed quadratic curvature in plots of $1/\Phi_{SiH}$ versus 1/[ROH]. If an intermediate complex is involved in these cases, as in Scheme 1, then the k_c pathway would have to be exclusively operative in the formation of the hydrosilanes. An alternate possibility is also compatible with the solvent polarity effect and quadratic curvature, that conversion of complex to hydrosilane is 100% efficient (k_{dc}

(10) (a) Griller, D.; Liu, M. T. H.; Scaiano, J. C. *J. Am. Chem. Soc.* **1982**, *104*, 5549. (b) Curvature is also pronounced in plots of decay rates of certain Si=C intermediates against acetic acid, which is known to form dimers: Kerst, C.; Rogers, C. W.; Ruffolo, R.; Leigh, W. J. *J. Am. Chem. Soc.* **1997**, *119*, 466.

(11) The derivation assumes the hydrosilane quantum yield $\Phi_{SiH} = \Phi_{12}\Phi_{2c}\Phi_{cp}$ where $\Phi_{12} = k_{12}\tau_1/(1 + k_{q1}\tau_1[\mathrm{MeOH}])$, $\Phi_{2c} = k_{q2}\tau_2[\mathrm{MeOH}]/(1 + k_{q2}\tau_2[\mathrm{MeOH}])$, and $\Phi_{cp} = (k_c\tau_c + k_{qc}\tau_c[\mathrm{MeOH}])/(1 + k_{qc}\tau_c[\mathrm{MeOH}])$. The rate constants are defined in Scheme 1. Inverting Φ_{SiH} and multiplying by 1/[MeOH]^3 furnishes eq 5. Note: $\tau_1^{-1} = k_{f1} + k_{d1} + k_{12}$, $\tau_2^{-1} = k_{f2} + k_{d2} + k_{r2}$, and $\tau_c^{-1} = k_{dc} + k_c$.

$\ll k_c + k_{qc}$[MeOH]). On the other hand, if dissociation of the complex is rapid such that $k_{dc} \gg k_{qc}$[MeOH], then eq 3 reduces to quadratic form and the solvent polarity dependent k_{12} would no longer be necessary to explain the quadratic behavior[1a,4] of $1/\Phi_{SiH}$ versus 1/[MeOH] in the case of the disilanes. Efficient dissociation of the complex to regenerate reactants could explain the low quantum yields for hydrosilane ($\Phi_{SiH} = 0.029$) observed for photolysis of (*E*)-**1** at high concentrations of MeOH, but a rapid electron transfer step with a rate constant k_{12} that is insensitive to solvent polarity may have difficulty accommodating the efficient ^{1}LE state *E,Z* isomerization in CH_2Cl_2 in this case.

The results of biacetyl-sensitized photolyses combined with azulene quenching rule against significant involvement of the ^{3}LE state in the *E,Z* photoisomerization of (*E*)-**3**. The distinction between CT and ^{3}LE states in *E,Z* photoisomerization cannot be made on the basis of the quenching by MeOH that is shown in Figures 5−7, because eqs 2−4 would still hold if the *E,Z* photoisomerization were to occur in the ^{3}LE state rather than the CT excited state. For the ^{3}LE state photoisomerization, it would only be necessary to redefine parameter *d*. As noted in the Results section, parameter *d* would then equate with $\Phi^\circ_{EZ} = \phi_{12}\phi_{23}\phi_{r3}$ (Scheme 1), which considers back electron transfer from the CT excited state as the most likely path for population of the ^{3}LE state. This definition neglects any contribution to population of the ^{3}LE state by intersystem crossing directly from the ^{1}LE state, which would likely be inefficient.[4,12] In any event, the azulene quenching results (Results Section) indicate that the same excited state is involved in both the *E,Z* photoisomerization and formation of hydrosilane **4** upon direct photolysis of (*E*)-**3**. This excited state cannot be the lowest triplet, because biacetyl triplet sensitized photolysis in 2 M MeOH in CH_2Cl_2 does not produce the hydrosilane, even though highly efficient *E,Z* photoisomerization is observed. Azulene is a well-known[13,14] quencher of stilbene singlet and triplet excited states.

Conclusion

Replacement of the disilanyl group of (*E*)-**1** with the 2-heptamethyltrisilanyl group of (*E*)-**3** increases the polarity of the CT excited state and significantly red-shifts the CT fluorescence maxima, as would be expected, considering that the trisilanyl group is the better electron donor.[15,16] Dual-sloped solvatochromic plots are observed for (*E*)-**1**[4] and (*E*)-**3** which suggest a ^{1}LE emission contributes to the overall fluorescence, particularly in relatively less polar ether solvents, whereas the dominant emissive excited state in intermediate polarity solvents such as CH_2Cl_2 is CT. Quenching of this emission by MeOH in CH_2Cl_2 results in a quadratic Stern−Volmer plot for (*E*)-**3**, consistent with quenching of two excited states, with the lower energy CT excited state the emissive excited state in CH_2Cl_2.

Like DCS,[17,18] (*E*)-**3** undergoes *E,Z* photoisomerization in the CT excited state in medium-polarity solvent, whereas the ^{1}LE state was found to be the reactive excited state in the case of (*E*)-**1**. The quadratic curvature observed in the Stern−Volmer plot for quenching of the isomerization by MeOH in CH_2Cl_2 was similar to that observed for fluorescence quenching. One of the $k_q\tau$ values is in good agreement with lifetime measurements of CT fluorescence at various MeOH concentrations.

Quenching of the *E,Z* isomerization by MeOH is accompanied by formation of hydrosilane **4**. Azulene quenching experiments show that the hydrosilane and the *E,Z* photoisomerization derive from the same excited state, which is assigned as the CT excited state. The variation of hydrosilane quantum yields with [MeOH] in CH_2Cl_2 correlates well with a mechanism involving complexation of the CT excited state with the MeOH, followed by a bimolecular rather than intramolecular reaction with MeOH to furnish the final product. Complexation is thought to involve nucleophilic interaction of the MeOH lone pair with an electron deficient silicon. Nucleophilic solvents such as THF effectively interact with the CT excited state, which results in quenching of the fluorescence and the *E,Z* isomerization.

Additional work is needed to establish the geometry of the intramolecular CT excited state of (*E*)-**3**. The very high quantum yield of fluorescence and correspondingly low *E,Z* photoisomerization efficiency of (*E*)-**3** in CH_2Cl_2 may reflect the greater stability of the more polar CT excited state relative to a less polar ^{1}p* excited state, as has been established for DCS.[17] A nonplanar geometry with respect to styryl and anilino groups was recently proposed to account for high fluorescence efficiencies and inefficient *E,Z* photoisomerizations of *m*-amino stilbenes, whereas the *p*-amino derivatives were thought to be essentially planar.[19] In the relaxed CT excited state of DCS, on the other hand, partial rotation about the trisilanylphenyl−cyanostyryl bond has been proposed,[18] and there is general agreement that rotation about the C−N bond is unimportant, in contrast to the TICT state of dimethylaminobenzonitrile.[17,18,20] If disilane (*E*)-**1**[4] is analogous to DCS, a TICT (alternately termed OICT[1a]) state involving C−Si bond rotation may not be applicable. The applicability of the TICT (OICT) concept in trisilanes bearing pendant electron acceptor substituents warrants further study to determine how the energy of the intramolecular CT excited state varies as a function of C−Si bond rotation.

Experimental Section

^{1}H NMR, ^{13}C NMR, and ^{2}H NMR spectra were recorded at 300, 75, and 46 MHz, respectively. GC-MS analyses were performed at 70 eV with a DB-1 capillary column (0.25 mm × 30 m, 0.25 μm film thickness), temperature programmed for 150 °C for 5 min and then 250 °C at 10 °C min^{-1}.

Silica gel (60−200 mesh, grade 62, 150 Å) was used for standard column chromatography. Medium-pressure liquid chromatography (MPLC) utilized a 82 cm × 2.5 cm column of 230−400 mesh silica gel (Merck grade 9385, 60 Å, Aldrich) with ether in hexane as eluant at a flow rate of 15 mL min^{-1}, unless specified otherwise below. Analytical HPLC utilized a

(12) Görner, H. *J. Photochem.* **1980**, *13*, 269.
(13) Saltiel, J.; Carlton, J. L. In *Rearrangements in Ground and Excited States*; de Mayo, P., Ed.; Organic Chemistry Series 42, Vol. 3, Essay 14; Academic: New York, 1980.
(14) Görner, H.; Kuhn, H. J. *Adv. Photochem.* **1995**, *19*, 1.
(15) Boberski, W. G.; Allred, A. L. *J. Organomet. Chem.* **1975**, *88*, 65−72.
(16) Bock, H.; Ensslin, W. *Angew. Chem., Int. Ed. Engl.* **1971**, *10*, 404.
(17) Il'ichev, Y. V.; Kühnle, W.; Zachariasse, K. A. *Chem. Phys.* **1996**, *211*, 441.
(18) Abraham, E.; Oberle, J.; Jonusauskas, G.; Lapouyade, R.; Rulliere, C. *Chem. Phys.* **1997**, *214*, 409.
(19) Lewis, F. D.; Yang, J.-S. *J. Am. Chem. Soc.* **1997**, *119*, 3834.
(20) Gruen, H.; Görner, H. *Z. Naturforsch.* **1983**, *38a*, 928.

14.6 mm × 250 mm column of 5 μm silica (Adsorbosil, Alltech). The flow rate was 1.5 mL min^{-1} with 0.8:10:100 by volume of ether:CH_2Cl_2:hexane as the mobile phase. UV detector response was calibrated by standard mixtures.

GC analyses were performed on an HP-5 capillary column (0.25 mm × 30 m, 0.25 μm film) temperature programmed at 70 °C for 4 min and then at 250 °C at 10 °C min^{-1}. Nitrogen was the carrier gas. Detector response was calibrated by standard mixtures.

Solvents were MeOH (EM Omnisolv, distilled from Mg), pentane (Baxter, high purity), hexane (Aldrich, HPLC), THF (Aldrich, 99.9%, anhydrous, refluxed and distilled from sodium and benzophenone), CH_3CN (Aldrich, HPLC, refluxed 3 days over CaH_2 and distilled), CH_2Cl_2 (Aldrich, HPLC, refluxed 3 h over CaH_2 and then distilled), $CHCl_3$ (Fisher, HPLC), CCl_4 (Aldrich, ACS), Et_2O (Aldrich, distilled from Na), and *n*-Bu_2O (Aldrich, distilled from Na).

Preparation of 4-(2′-Heptamethyltrisilanyl)benzonitrile. The procedure was similar to that reported for generation of lithiobenzonitriles and reaction with electrophiles.[21] To a solution of 3.4 g (18.4 mmol) of 4-bromobenzonitrile in 150 mL of anhydrous THF at −78 °C was added dropwise via syringe 7.5 mL (18.8 mmol) of 2.5 M *n*-butyllithium in hexane with stirring under nitrogen. After 10 min, 4.0 g (17.9 mmol) of 2-chloroheptamethyltrisilane[22] was added via syringe. After stirring the reaction mixture for 40 min at −78 °C, 5 mL of MeOH and 20 mL of water were added, and the mixture was allowed to warm slowly to room temperature. The reaction mixture was extracted three times with 30 mL portions of ether. The combined extracts were washed with saturated NH_4Cl, twice with 50 mL of water, dried over anhydrous Na_2SO_4, and concentrated in vacuo to give a brown oil. Standard column chromatography eluting with 2% ether in hexane gave 3.6 g of product as an oil, which was ca. 70% pure by GC-MS analysis. This material was used without further purification in the synthesis of 4-(2′-heptamethyltrisilanyl)benzaldehyde. The synthesis was repeated to obtain a sample for further purification. However, attempts to obtain an analytically pure sample by repeated standard chromatography, eluting with 2% ether in hexane, failed. The spectral data of ca. 95% pure material were as follows: ^{1}H NMR ($CDCl_3$) δ 0.105 (s, 18 H, CH_3), 0.387 (s, 3 H, CH_3), 7.47 (d, J_{AX} = 8.0 Hz, 2 H, aromatic), 7.55 (d, J_{AX} = 8.0 Hz, 2 H, aromatic); GC-MS *m*/*z* (relative intensity) 291 (28), 276 (5), 73 (100).

Preparation of 4-(2′-Heptamethyltrisilanyl)benzaldehyde. To a solution of 3.6 g (12.4 mmol) of 4-(2′-heptamethyltrisilanyl)benzonitrile in 40 mL of CH_2Cl_2, cooled under nitrogen with an ice bath, was added via syringe 12.5 mL of 1 M diisobutylaluminum hydride in hexane. The mixture was stirred 4−5 h at room temperature. After addition of 5 mL of EtOH, dilute aqueous HCl was added, and the mixture was extracted three times with 20 mL of ether. The combined ether extracts were washed once with 30 mL of saturated $NaHCO_3$ and twice with 30 mL of water, dried over anhydrous Na_2SO_4, and concentrated in vacuo to give a yellow oil. Standard column chromatography eluting with 2% ether in hexane gave 2.0 g of ca. 70% pure aldehyde, as an oil, which was used without further purification in the synthesis of the trisilanyl cyanostilbene (vide infra). The synthesis was repeated to obtain a sample for further purification. Standard chromatography was performed twice, eluting with 2% ether in hexane, to obtain ca. 90% pure product containing *p*-trimethylsilylbenzaldehyde as the major impurity, according to GC-MS analysis. The spectral data of this sample were as follows: ^{1}H NMR ($CDCl_3$) δ 0.116 (s, 18 H, CH_3), 0.416 (s, 3 H, CH_3), 7.55 (d, J_{AX} = 8.2 Hz, 2 H, aromatic), 7.78 (d, J_{AX} = 8.2 Hz, 2 H, aromatic), 9.99 (s, 1 H, CHO); GC-MS *m*/*z* (relative intensity) 294 (4), 73 (100).

Preparation of (*E*)-4-Cyano-4′-(2″-heptamethyltrisilanyl)stilbene (*E*)-3. The procedure was similar to that reported for the synthesis of *trans*-stilbene.[23] A mixture of 4.0 g (20 mmol) of *p*-cyanobenzylbromide and 3.7 g (22 mmol) of triethyl phosphite was heated to reflux for 4 h to give a colorless oil, which GC-MS analysis showed to be *p*-cyanobenzyldiethyl phosphite. A 2.15 g (8.50 mmol) portion of the phosphite was dissolved in 5 mL of anhydrous DME and added dropwise to a suspension of 290 mg (7.25 mmol) of NaH (60% in mineral oil) at room temperature under nitrogen, followed by addition of 2.0 g (6.8 mmol) of 70% pure 4-(2′-heptamethyltrisilanyl)-benzaldehyde in 5 mL of anhydrous DME. Upon slow heating of the mixture, gas evolution was observed. After 30 min at reflux, 5 mL of water was added, and the mixture was extracted three times with 20 mL portions of ether. The combined ether extracts were washed twice with 20 mL of water, dried over anhydrous Na_2SO_4, and concentrated in vacuo to give a yellow oil. Standard chromatography eluting with 2% ether in hexane gave 1.5 g of 80% pure product by GC-MS analysis, as a yellow solid. Recrystallization from absolute ethanol gave 0.9 g (48% yield) of analytically pure product, mp 117.5−118 °C. The spectral data were as follows: ^{1}H NMR ($CDCl_3$) δ 0.120 (s, 18 H, CH_3), 0.391 (s, 3 H, CH_3), 7.10 (d, J_{AB} = 16 Hz, 1 H, C═CH), 7.20 (d, J_{AB} = 16 Hz, 1 H, C═CH), 7.41 (d, J_{AB} = 8.0 Hz, 2 H, aromatic), 7.46 (d, J_{AB} = 8.0 Hz, 2 H, aromatic), 7.58 (d, J_{AB} = 8.4 Hz, 2 H, aromatic), 7.64 (d, J_{AB} = 8.4 Hz, 2 H, aromatic); ^{13}C NMR ($CDCl_3$) δ −8.48, 0.44, 111.04, 119.80, 126.77, 127.01, 127.49, 133.17, 133.24, 135.55, 136.19, 140.13, 142.63. GC-MS *m*/*z* (relative intensity) 393 (29), 378 (24), 320 (60), 73 (100). Anal. Calcd for $C_{22}H_{31}NSi_3$: C, 67.11; H, 7.94; N, 3.56. Found: C, 66.90; H, 7.86; N 3.68.

Preparative Direct Photolyses. A solution of 180 mg (0.46 mmol) of (*E*)-**3** in 75 mL of MeOH contained in a Pyrex tube sealed by a rubber septum was purged with nitrogen for 30 min and irradiated for 15 min beside a water-cooled, jacketed Hanovia 450-W medium-pressure mercury lamp equipped with a Pyrex filter. Standard column chromatography (vide supra) eluting with 1.5% ether in hexane gave 46 mg (0.14 mmol, 31%) of *trans*-hydrosilane **4** as an analytically pure, colorless crystalline solid, mp 71−72 °C. The next fraction was 66 mg of a colorless solid containing 79% of *trans*-**4**, 7.3% of *cis*-**4**, and 11% of reactant (*E*)-**3**, according to GC-MS analysis. The final fraction was 30 mg (0.064 mmol, 20% yield) of the cis isomer of hydrosilane **4** as a colorless oil.

A solution of 120 mg (0.305 mmol) of (*E*)-**3** in 60 mL of CH_2Cl_2 was irradiated for 30 min using the above procedure. Standard column chromatography eluting with 1% ether in hexane and then 2% ether in hexane gave 35 mg (0.089 mmol, 29% recovery) of reactant (*E*)-**3**. The next fraction collected was 80 mg (0.207 mmol, 67%) of (*Z*)-**3**, as a colorless oil.

The spectral data and elemental analysis of the trans isomer of hydrosilane **4** were as follows: ^{1}H NMR ($CDCl_3$) δ 0.121 (s, 9 H, CH_3), 0.424 (d, J_{AX} = 4.5 Hz, 3 H, CH_3), 4.20 (q, J_{AX} = 4.5 Hz, 1 H, SiH), 7.11 (d, J_{AB} = 16.4 Hz, 1 H, C═CH), 7.21 (d, J_{AB} = 16.4 Hz, 1 H, C═CH), 7.49 (s, 4 H, aromatic), 7.58 (d, J_{AB} = 8.7 Hz, 2 H, aromatic), 7.64 (d, J_{AB} = 8.7 Hz, 2 H, aromatic); ^{13}C NMR ($CDCl_3$) δ −7.49, −1.21, 111.22, 119.72, 126.92, 127.45, 127.53, 133.08, 133.16, 135.80, 137.09, 137.91, 142.50. GC-MS *m*/*z* (relative intensity) 321 (76), 306 (26), 73 (100). Anal. Calcd for $C_{19}H_{23}NSi_3$: C, 70.97; H, 7.21; N, 4.36. Found: C, 70.84; H, 7.27; N, 4.43.

The spectral data of the cis isomer of hydrosilane **4** were as follows: ^{1}H NMR ($CDCl_3$) δ 0.097 (s, 9 H, CH_3), 0.388 (d, J_{AX} = 4.7 Hz, 3 H, CH_3); 4.16 (q, J_{AX} = 5.0 Hz, 1 H, SiH), 6.56 (d, J_{AX} = 11.8 Hz, 1 H, C═CH), 6.74 (d, J_{AX} = 12.3 Hz, 1 H, C═CH), 7.14 (d, J_{AX} = 8.1 Hz, 2 H, aromatic), 7.32 (d, J_{AX} = 8.3 Hz, 2 H, aromatic), 7.35 (d, J_{AX} = 8.1 Hz, 2 H, aromatic), 7.50 (d, J_{AX} = 8.3 Hz, 2 H, aromatic); GC-MS *m*/*z* (relative intensity) 321 (82), 306 (23), 73 (100).

The spectral data for (*Z*)-**3** were as follows: ^{1}H NMR ($CDCl_3$) δ 0.102 (s, 18 H, CH_3), 0.361 (s, 3 H, CH_3), 6.54 (d, J_{AX} = 12 Hz, 1 H, C═CH), 6.76 (d, J_{AX} = 12 Hz, 1 H, C═CH), 7.12 (d,

(21) Parham, W. E.; Jones, L. D. *J. Org. Chem.* **1976**, *41*, 1187.
(22) Kumada, M.; Ishikawa, M.; Maeda, S. *J. Organomet. Chem.* **1964**, *2*, 478.
(23) Wadsworth, W. S.; Emmons, W. D. *J. Am. Chem. Soc.* **1961**, *83*, 1733.

J_{AX} = 7.7 Hz, 2 H, aromatic), 7.27 (d, J_{AX} = 7.7 Hz, 2 H, aromatic), 7.31 (d, J_{AX} = 8.0 Hz, 2 H, aromatic), 7.48 (d, J_{AX} = 8.5 Hz, 2 H, aromatic); GC-MS *m/z* (relative intensity) 393 (40), 378 (34), 320 (76), 290 (14), 73 (100).

Photolyses with MeOD. The general procedure for quantum yield determinations was used (vide infra). Two samples of 50 mg (0.17 mmol) of (*E*)-**3** in 12.5 mL of either MeOD or 3 M MeOD in CH_2Cl_2 as the solvent were irradiated at 340 nm for 2 h (ca 3−5% conversion). After concentration in vacuo and dissolution in CH_2Cl_2, each photolysate was analyzed by GC-MS. In addition to undeuterated (*E*)-**3**, deuterated hydrosilane **4** was observed; (*Z*)-**3** was not analyzed due to its low yield. The M − 15 fragment ion of deuterated **4** was used to calculate the isotopic distribution, because a prominent M − 1 fragment ion was observed for undeuterated **4**, invalidating analysis of the parent ion.[24] The isotopic distributions are summarized in the Results section. The sample from the MeOD run was reconcentrated and dissolved in CCl_4, and ^{2}H NMR analysis showed only a single peak at δ 4.3−4.4.

Quantum Yields of Fluorescence in Various Solvents. The fluorescence spectra were measured at 330 nm excitation wavelength in each solvent at concentrations below 10^{-5} M such that the absorbances were < 0.1. A 1 N H_2SO_4 solution of quinine bisulfate served as the standard (Φ_f = 0.546).[25a−c] Samples were not deaerated. The quantum yields were calculated from the equation $\Phi_u = [(A_s F_u n_u^2)/(A_u F_s n_s^2)]\Phi_s$,[25d] where Φ is the quantum yield of fluorescence, *A* is absorbance, *F* is the integrated emission across the band, *n* is refractive index of the solvent, u stands for unknown, s pertains to standard. The quantum yields (Φ_f) are given in Table 2.

Dependence of Relative Quantum Yields of Fluorescence in Pentane and CH_2Cl_2 on MeOH Concentration. Fluorescence spectra of 1.27 × 10^{-4} M solutions of (*E*)-**3** were measured at 340 nm excitation wavelength in each solvent at various concentrations of MeOH. The integrated area under the fluorescence peak was considered proportional to Φ_f with $\Phi°_f$ the integrated emission for zero [MeOH]. The data for MeOH in CH_2Cl_2 were as follows (Figure 3): $\Phi°_f/\Phi_f$ ([MeOH]/M), 1.00 (0.0), 3.00 (2.0), 4.71 (4.0), 6.89 (6.1), 11.0 (8.3), 14.4 (9.8). The data for MeOH in pentane were as follows: $\Phi°_f/\Phi_f$ ([MeOH]/M), 1.00 (0.0), 1.99 (2.0), 3.12 (3.9), 4.00 (6.0), 5.00 (8.0).

Singlet Excited State Lifetimes. The single photon counting lifetime apparatus and procedure for lifetime measurements have been previously described.[4] The χ^2 test and the Durbin−Watson (DW) parameter were used as statistical tests to judge the quality of fitted decays. Satisfactory monoexponential fits of decays were obtained.

The lifetimes in Table 2 were determined for samples of 1.6−4.6 × 10^{-5} M (*E*)-**3** in various solvents. Each sample was purged with nitrogen for 30 min and sealed with a Teflon stopcock. The excitation wavelength was 337 nm, and two determinations (average deviation ≤ 0.1 ns) were made at the emission maximum for each solvent. For CH_2Cl_2 as the solvent the lifetime measured near the onset (395 nm) was τ = 1.50 ± 0.04 ns, and at the maximum of the emission band (453 nm) τ = 1.65 ± 0.05 ns.

Lifetimes τ were determined for 1.9 × 10^{-5} M solutions of (*E*)-**3** in CH_2Cl_2 containing various concentrations of MeOH. The mean for four determinations at each concentration are summarized as follows [τ, ns ([MeOH])]: 1.6 ± 0.1 (0.0), 0.92 ± 0.05 (1.0), 0.63 ± 0.04 (2.0), 0.46 ± 0.04 (3.0), 0.41 ± 0.03 (4.0), 0.31 ± 0.06 (5.0). The data are plotted in Figure 4.

General Procedure for Product Quantum Yield Determinations. The semimicro optical bench for quantum yield determinations is similar to the apparatus described by Zimmerman.[26] Light from a 200 W high-pressure mercury lamp was passed through an Oriel monochromator with entrance and exit slits set to 3 mm to give a 20 nm band-pass fwhm, collimated through a lens, and 17% was diverted by a beam splitter to a cell containing actinometer, perpendicular to the light path. The photolysate in a 5 cm × 1.8 cm quartz cylindrical cell of 12.5 mL volume was mounted in-line with the optics, monochromator, and lamp. Light output was monitored by ferrioxalate actinometry,[27] using the splitting ratio technique.

Photolysates were purged by nitrogen for 30 min prior to irradiation. Conversions were kept below 5%. The products were quantified by GC (vide supra). The GC retention times were as follows: 24.7 min docosane standard, 34.6 min (*Z*)-**3**, 35.8 min hydrosilane **4**, and 53.6 min (*E*)-**3**.

Quantum yields Φ_{EZ} in various solvents are summarized in Table 2. Additional quantum yields are given below.

Quantum Yields in CH_2Cl_2 Containing MeOH. Data for 340 nm direct photolyses of 0.01 M (*E*)-**3** were as follows: $\Phi_{E,Z}$ ([MeOH], M), 0.202 (0), 0.133 (0.50), 0.117 (0.60), 0.104 (0.80), 0.0899 (1.0), 0.0624 (1.4), 0.0523 (2.0), 0.0226 (4.0). Φ_{SiH} ([MeOH]), 0.0278 (0.80), 0.0364 (1.0), 0.0512 (1.4), 0.0756 (2.0), 0.106 (4.0), 0.122 (8.0). The data were used to construct Figures 5−7.

Quantum Yields with Azulene Quencher. Following the general procedure for quantum yield determinations, nitrogen-purged solutions of 0.01 M (*E*)-**3** in 2.0 M MeOH in CH_2Cl_2 containing various concentrations of azulene were irradiated at 380 nm. The quantum yields were as follows: Φ_{EZ} ([azulene], M), 0.0485 (0.0), 0.0417 (0.0050), 0.0379 (0.010), 0.0348 (0.015), 0.0325 (0.020); Φ_{SiH} ([azulene], M), 0.0885 (0.0), 0.0826 (0.0050), 0.0800 (0.010), 0.0676 (0.015), 0.0610 (0.020). The data were used to construct Figure 8.

Biacetyl Sensitized Photolyses. Following the general procedure for quantum yield determinations, a nitrogen-purged solution of 0.05 M biacetyl and 0.01 M (*E*)-**3** in CH_2Cl_2 was irradiated at 430 nm. The biacetyl absorbed > 99.9% of the light. After irradiation, fluoanthene was added as internal standard, the photolysate was concentrated in vacuo, and CH_2Cl_2 was added. The products were quantified by HPLC analysis using a standard mixture of fluoranthene (retention time 9.6 min), (*Z*)-**3** (20 min), and hydrosilane **4** (31 min). The photolysate showed (*E*)-**3** at 27 min, no hydrosilane **4** was detected, and (*Z*)-**3** was formed with a quantum yield of 0.42. With 5 M MeOH in CH_2Cl_2 as the solvent, the quantum yield for (*Z*)-**3** was 0.41.

Acknowledgment. Financial support of this work by NSF (CHE-9407036) and by the Committee on Research, Marquette University, is gratefully acknowledged.

JO982378+

(24) Biemann, K. In *Mass Spectrometry*; McGraw-Hill: New York, 1962; p 209.

(25) (a) Meech, S. R.; Phillips, D. *J. Photochem.* **1983**, *23*, 193. (b) Hamai, S.; Hirayama, F. *J. Phys. Chem.* **1983**, *87*, 83. (c) Melhuish, W. H. *J. Phys. Chem.* **1961**, *65*, 229. (d) Eaton, D. F. In *Handbook of Organic Photochemistry*; Scaiano, J. C., Ed.; Vol. I; CRC Press: Boca Raton, FL, 1989; Chapter 8.

(26) Zimmerman, H. E. *Mol. Photochem.* **1971**, *3*, 281.

(27) Hatchard, C. G.; Parker, C. A. *Proc. R. Soc. London* **1956**, *235*, 518.